

# Investigating Adsorption Behaviour of Cobalt Vanadate Nanocomposites on Methylene Blue Dye

Monika<sup>a</sup>, Virender Kumar<sup>a</sup>, Prashant Kumar<sup>b</sup>, Ravinder Kumar<sup>c</sup>, Vijay Kumar Goel<sup>a\*</sup> & Vinod Kumar<sup>b\*</sup>

<sup>a</sup>Department of Chemistry, School of Physical Sciences, Jawaharlal Nehru University, New Delhi 110067, India

<sup>b</sup>Special Centre for Nano Science, Jawaharlal Nehru University, Delhi 110 067, India

<sup>c</sup>Department of chemistry, Gurukula Kangri (Deemed to be University), Haridwar, UK 249 404 India

Received 3 July 2023; accepted 4 August 2023

( $\alpha$ ,  $\beta$ )- $\text{CoV}_3\text{O}_8/\text{V}_4\text{O}_7$  nanocomposites have been successfully synthesized through a facile hydrothermal method at low temperature. The structural properties of these nanocomposites are characterized via Powder X-ray diffraction, Fourier Transform Infrared spectroscopy (FTIR), Scanning electron microscopy (SEM), and X-ray energy dispersive spectroscopy (EDX) analysis. Synthesized nanocomposites were determined to have an approximate crystalline size of 3.72 nm, and SEM imaging exhibited aggregated irregular rectangular shaped nanocomposites. Adsorption kinetics and isotherms were examined, and the outcomes showed that the adsorption followed pseudo-second-order kinetic model and Langmuir isotherm. Adsorption of methylene blue dye was investigated using ( $\alpha$ ,  $\beta$ )- $\text{CoV}_3\text{O}_8/\text{V}_4\text{O}_7$  nanocomposites at varying concentrations of the dye. 20  $\mu\text{M}$  aqueous solution of methylene blue was found to have a high adsorption efficiency of almost 95% in 5 minutes.

**Keywords:** Methylene blue; FTIR; Adsorption kinetics; Nanocomposites

## 1 Introduction

Dye effluent from industrial processes is a major source of water contamination and a contributor to the world's pollution crisis<sup>1</sup>. Dyes have multiple benefits, including textile, printing, food, and cosmetics<sup>2,3</sup>. Despite their numerous benefits, dyes have highly deleterious effects on the environment and human health. Methylene blue (MB) is a common cationic dye toxic to humans and the environment at high concentrations<sup>4</sup>. Dye removal, degradation, and toxicity reduction often use a combination of physical, chemical, biological, and thermal processes<sup>5</sup>. Metal oxide nanoparticles are utilized as a catalyst to improve nanotechnology-based methods for removing and treating hazardous cationic dyes. Transition metal oxides have drawn attention for a variety of applications due to their unique physiochemical characteristics. ( $\alpha$ ,  $\beta$ )- $\text{CoV}_3\text{O}_8/\text{V}_4\text{O}_7$  nanocomposites are mostly used photocatalytic degradation of cationic dyes whereas in this work these nanoparticles show adsorption properties of MB dye. Synthesis of nanocomposites via hydrothermal method is simple, low-cost and environment friendly. It produces aligned and

ordered nanostructures. Adsorption is employed for removal of dye and there are several factors affecting this such as adsorbent dose, temperature and pH effect. Using analytical methods such as PXRD, SEM, and UV-Visible spectroscopy, the adsorption effectiveness for MB dye of hydrothermally produced ( $\alpha$ ,  $\beta$ )- $\text{CoV}_3\text{O}_8/\text{V}_4\text{O}_7$  nanocomposites is utilized for treatment of wastewater.

## 2 Materials and Methods

$\text{Co}(\text{NO}_3)_2 \cdot 6\text{H}_2\text{O}$  (>99% purity, Emsure Merck),  $\text{VCl}_3$  (>97% purity, TCI), PEG(Merck), and MB (Thermo Fisher Scientific) were procured. For the purpose of conducting experiments, 1000  $\mu\text{M}$  MB stock solution was prepared and further diluted to achieve the desired  $\mu\text{M}$  levels. The hydrothermal approach was used to synthesize ( $\alpha$ ,  $\beta$ )- $\text{CoV}_3\text{O}_8/\text{V}_4\text{O}_7$  nanocomposites from  $\text{Co}(\text{NO}_3)_2 \cdot 6\text{H}_2\text{O}$  (0.50 M) and  $\text{VCl}_3$  (0.30 M). Both of the aforesaid compounds were dissolved in a small amount of water before being with 50 ml of polyethylene glycol (PEG) as a solvent. To homogenize the mixture, agitate it for 15 minutes using a magnetic stirrer. The solution is then transferred to a Teflon vessel, packed in an autoclave, and placed in oven for 15 hours at 150 °C. Autoclave was cooled to room temperature before filtering and washing it 3-4 times with water to remove any

\*Corresponding authors:  
(E-mail: vijaykgoel@mail.jnu.in; kumarv@mail.jnu.ac.in)

impurities. The sample was dried at 120 °C for 12 hours, yielding a greenish-black powder.

### 3 Results and Discussion

#### 3.1 X-ray diffraction

The PXRD pattern has been shown in Fig. 1. The synthesised nanocomposites exhibits orthorhombic phase,  $\alpha$ - $\text{CoV}_3\text{O}_8$  with space group  $Ibam$  (72) and monoclinic phase,  $\beta$ - $\text{CoV}_3\text{O}_8$  with space group  $C2/m$  (12) are in agreement to JCPDS file No. 22-0598 and 22-0599 respectively<sup>6</sup>. The X-ray pattern has characteristic planes (001), (211), (222), (303), (040), (701), and (134)<sup>7</sup>. The high intensity peaks at (211), (222), and (303) corresponds to formation of  $\alpha$ - $\text{CoV}_3\text{O}_8$ <sup>6</sup>. The phase of  $\text{V}_4\text{O}_7$  was found to be in primitive lattice with space group  $P\bar{1}(2)$  which corresponds to JCPDS file No.65-6448. This analysis confirms that ( $\alpha$ ,  $\beta$ )- $\text{CoV}_3\text{O}_8/\text{V}_4\text{O}_7$  nanocomposites were successfully formed via the hydrothermal method. Debye-Scherrer equation was utilized to determine the average crystalline size of nanocomposites from PXRD, which was 3.72 nm.

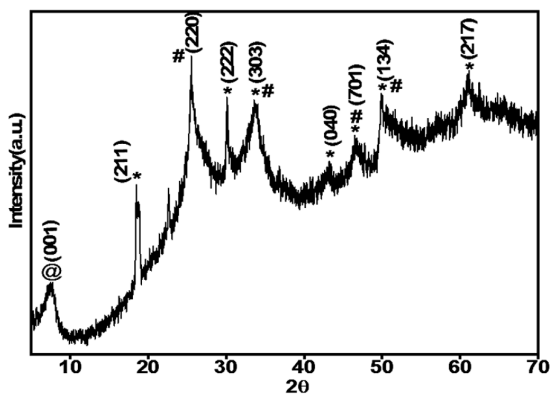


Fig. 1 — PXRD pattern of ( $\alpha$ ,  $\beta$ )- $\text{CoV}_3\text{O}_8/\text{V}_4\text{O}_7$  nanocomposites, where (\*) shows  $\alpha$ - $\text{CoV}_3\text{O}_8$  phase, (#) describes  $\beta$ - $\text{CoV}_3\text{O}_8$  phase and (@) shows  $\text{V}_4\text{O}_7$  phase.

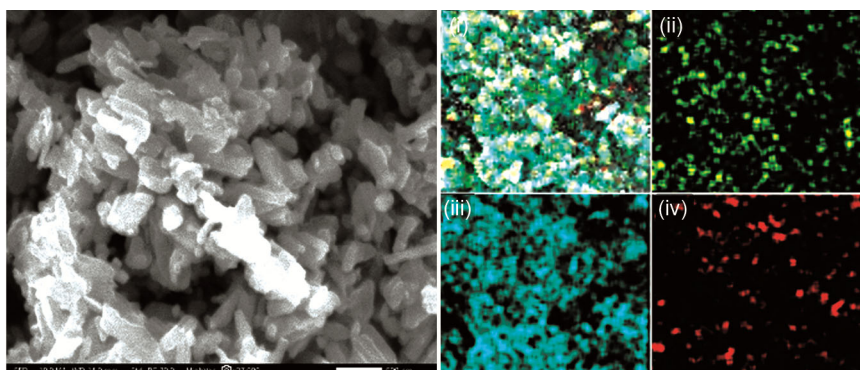


Fig. 2 — SEM image of ( $\alpha$ ,  $\beta$ )- $\text{CoV}_3\text{O}_8/\text{V}_4\text{O}_7$  nanocomposites and elemental mapping of synthesized nanocomposites illustrates (i) ( $\alpha$ ,  $\beta$ )- $\text{CoV}_3\text{O}_8/\text{V}_4\text{O}_7$  nanocomposites, (ii) Co as green colour, (iii) V as blue colour, (iv) O as red colour.

#### 3.2 SEM Analysis

The morphological studies of different sizes of sample particles have been characterized by SEM. Fig. 2(A), describes aggregated irregular rectangular shaped nanocomposites. Additionally, elemental composition and uniformity of Co, V and O in nanocomposites has been validated.

#### 3.3 FTIR Studies

The FTIR analysis was obtained to analyse different stretching frequencies in ( $\alpha$ ,  $\beta$ )- $\text{CoV}_3\text{O}_8/\text{V}_4\text{O}_7$  nanocomposites which represents strong peaks at  $1102\text{ cm}^{-1}$ ,  $990\text{ cm}^{-1}$  and  $508\text{ cm}^{-1}$  in Fig. 3. Strong peak at  $757\text{ cm}^{-1}$  represented stretching frequency of V-O and peak at  $983\text{ cm}^{-1}$  describes stretching frequency of V=O bond<sup>8</sup>. The stretching frequency of Co-O is around  $508\text{ cm}^{-1}$ . The stretching frequency at higher range around  $500\text{--}700\text{ cm}^{-1}$  belongs to tetrahedral site of metal whereas range around  $400\text{ cm}^{-1}$  depicts octahedral site of metal<sup>9,10</sup>.

#### 3.4 UV-Visible Spectroscopy

The nanocomposites completely adsorbed the dye, changing the solution from blue to transparent. 0.05 g of nanocomposites in 50 ml of aqueous dye solutions were evaluated with varied dye concentrations. Fig. 4, shows efficient adsorption of MB dye by ( $\alpha$ ,  $\beta$ )- $\text{CoV}_3\text{O}_8/\text{V}_4\text{O}_7$  nanocomposites, which resulted in nearly 95% adsorption within 5 minutes. This high rate of adsorption may be credited to the large surface area of aggregated irregular rectangular shaped nanocomposites, as confirmed through XRD and SEM results. The removal or adsorption efficiency ( $\eta$ ) has been calculated using the Eq. 1:

$$\eta = [(C_o - C_t)/C_o] \times 100 = [(A_o - A_t)/A_o] \times 100 \quad \dots (1)$$

Here,  $C_0$  and  $C_t$  are concentrations at  $t=0$  and at time  $t$ , respectively.  $A_0$  and  $A_t$  correspond to initial absorbance and absorbance after time  $t$ <sup>11</sup>.

**3.5 Adsorption Kinetics**

In order to determine the governing mechanism of adsorption processes, pseudo-first-order and pseudo-second-order kinetic models were used Fig. 5, illustrates that pseudo-first-order kinetic didn't fit well. In fact, the pseudo-second-order equation produced an excellent match to the

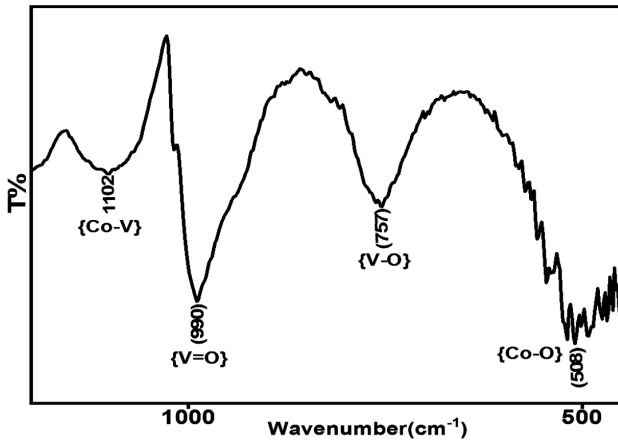


Fig. 3 — FTIR data of produced  $(\alpha, \beta)$ - $\text{CoV}_3\text{O}_8/\text{V}_4\text{O}_7$  nanocomposites.

experimental data, with regression coefficient of  $R^2$  values over 0.99%.

**3.6 Adsorption Isotherms**

In this investigation, the Freundlich and Langmuir adsorption isotherms were implemented. The Freundlich isotherm is used for a heterogeneous surface energy system. The Langmuir isotherm follows up homogeneous surface energy system<sup>12</sup>. Fig. 6, depicts

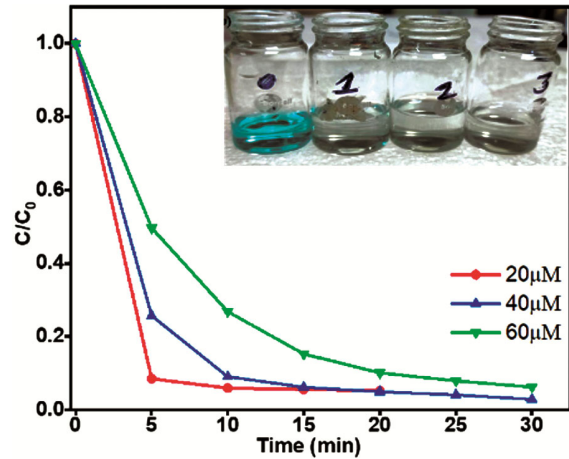


Fig. 4 — Adsorption of MB dye under various concentrations (red for 20 $\mu\text{M}$ , blue for 40 $\mu\text{M}$ , green for 60 $\mu\text{M}$ ), inset image depicts complete decolorization of MB dye at different time intervals.

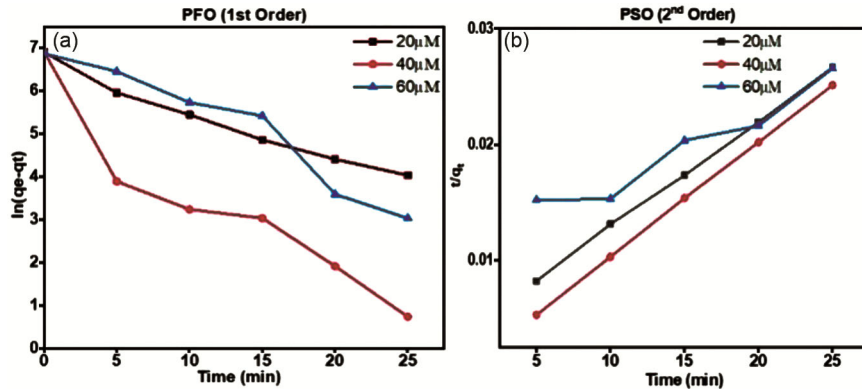


Fig. 5 — Plots of  $\ln(q_e - q_t) v/s t$  and  $t/q_t v/s t$  depicts the pseudo-first order kinetics and pseudo-second order kinetics respectively.

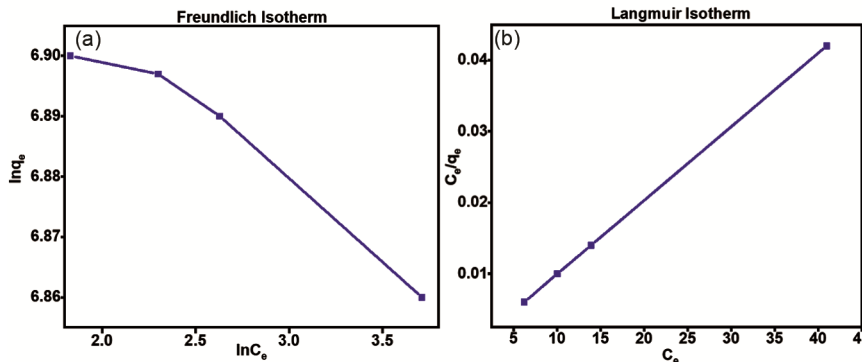


Fig. 6 — Plots of  $\ln q_e v/s \ln C_e$  and  $C_e/q_e v/s C_e$  describes Freundlich isotherm and Langmuir isotherm respectively.

that Langmuir isotherm fits better with  $R^2$  value of 0.99% from experimental analysis.

#### 4 Conclusion

This study is intended to demonstrate the Synthesis of ( $\alpha$ ,  $\beta$ )- $\text{CoV}_3\text{O}_8/\text{V}_4\text{O}_7$  nanocomposites. The aggregated irregular rectangular-shaped nanocomposites have found to be of average crystalline size 3.72 nm. Furthermore, UV-Visible based adsorption studies have proven the use of synthesized nanocomposites for the removal of MB dye from its aqueous solution. At  $20\mu\text{M}$  MB concentration, the adsorption efficacy of 95 % is obtained within 5 minutes. The mechanism for adsorption includes electrostatic attraction,  $\pi$ - $\pi$  interactions, as well as H-bonding interactions. The experimental data governs that it best fits pseudo-second-order kinetic model and Langmuir isotherm.

#### Acknowledgement

One of the author Monika thanks CSIR (File no. 09/0263(15268)/2022-EMR-I) for JRF and VKG thanks Sanganeria Foundation.

#### References

- 1 Kumar S, *et al*, *J Phys Chem C*, 127 (2023) 7095.
- 2 Muthukumaran C, *et al*, *J Taiwan Inst Chem Eng*, 63 (2016) 354.
- 3 Khan K, *et al*, *Water (Switzerland)*, 14 (2022) 242.
- 4 Sun L, *et al*, *Int J Environ Res Public Health*, 16 (2019) 4773.
- 5 Gusain R, *et al*, *Adv Colloid Interface Sci*, 272 (2019) 102009.
- 6 Jeong G H, *et al*, *Nanotechnology*, 29 (2018) 195403.
- 7 Casalo A P, *et al.*, *J Inorg.Nucl Chem*, 31 (1969) 3049.
- 8 O'Dwyer C, *et al*, *J Electrochem Soc*, 154 (2007) K29.
- 9 Celik G, *et al*, *Acta Phys Pol A*, 121 (2012) 203.
- 10 Hafeez M, *et al*, *Mater Res Express*, 7 (2020) 025019.
- 11 Imessaoudene A, *et al.*, *Separations*, 10 (2023) 10010057.
- 12 Ahmad A, *et al.*, *Bioresour Technol*, 306 (2020) 123202.